

Condition Based Maintenance Technology Development for Nuclear Control and Instrumentation (C&I) Cable via Korea-Hungary Joint Research

Final report (Project ID: 123672)

Principal Investigator: Zoltán Ádám Tamus

1 Background

Although the share of renewable sources is increasing in electrical energy generation, nuclear power plants (NPPs) still produce 10% of the total electricity worldwide. In addition, the lifetime extension of the existing fleet of NPPs has a crucial role in the cost-effective path to the decarbonisation of the electricity sector [1]. Therefore it is necessary to ensure existing nuclear power plants can operate as long as they are safe, supporting new nuclear construction and encouraging new nuclear technologies to be developed [2]. Long-term, safe operation of nuclear facilities relies on safety-related equipment, including cables, which have to fulfil their function in normal operation and all postulated events (design basis events — DBE) during their qualified lifetime. The purpose of cable condition monitoring in nuclear facilities is to determine whether cables remain in a qualified condition by monitoring one or more condition indicators [3]. The condition indicator should be measurable, change monotonically with time, and correlate with safety function performance under DBE conditions, showing a consistent trend from unaged through the limit of the qualified pre-accident condition. In the broadest terms, the condition monitoring methods can be classified into four groups, namely visual, electrical, mechanical and chemical techniques [4]. In the nuclear industry, the 50% elongation at break (EaB) value is traditionally considered an end-of-life criterion for polymer components, jackets and insulation of cables [5]. The measurement of EaB is also widely applied for determining the remaining lifetime [6]. However, this method, like other mechanical and chemical tests, has a significant drawback: samples must be taken from the cable insulation or jacket for the testing, i.e. it is a destructive test method.

Based on this background, the project's main goal was to develop a non-destructive condition monitoring method to support the maintenance of nuclear power plant (NPP) instrumentation and control (I&C) cables.

2 Research

During the operation in the NPP environment, the cables' polymeric components are exposed to several stresses, such as elevated temperature, radiation, mechanical bending or manipulation and chemical contamination [7, 8]. Since the subject of the investigation is low voltage (LV) I&C cables, the electrical stress can be negligible. Due to these stressors, the structure of polymeric materials changes by chain scission, cross-linking and oxidation. The alteration in the material structure results in a change in electrical, mechanical and chemical properties.

Since the non-destructivity is one of the key concerns from the practical applicability point of view, the research focused on the measurement of dielectric properties of cable insulation and jacket. Therefore, dielectric properties (complex permittivity, tan delta, capacitance) were measured in a wide frequency range from mHz to 500 kHz. Below the kHz range, an OMICRON Dirana dielectric spectrometer, for higher frequencies up to 500 kHz, a Wayne-Kerr 6430A impedance analyser, was used. Besides the frequency-domain measurements, a voltage response (VR) meter was developed to investigate the time-domain dielectric response.

Other non-electrical, possible non-destructive tests are based on indentation hardness testing. Because during functionality (Loss of Coolant Accident — LOCA) tests, the mechanical parameters have particular importance since cracks and ruptures appear in the jacket and insulation due to the loss of their flexibility, leading to short circuits between the conductors or shielding. Therefore the mechanical parameters were also tested by Shore D hardness measurement. As previously mentioned, the EaB measurement has an important role in evaluating the condition of polymeric components in NPPs hence the EaB was also measured. The correlation between the mechanical properties and the electrical parameters was also analysed, and the most reliable diagnostic markers were selected.

2.1 Equipment development

Within the project, a new voltage response meter was developed, implementing the extended voltage response method (EVR). The newly developed instrument has also been adapted to measure material samples, eliminating the difficulty of measuring the relatively small capacity of insulating material samples. In addition, a method has been developed to determine the dielectric response function from the results of EVR measurements [9].

The key component of the EVR meter is the electrostatic voltmeter, ensuring high input impedance of the equipment. The supplier could only deliver this instrument with an extreme delay, which meant that the development of the equipment could not be fully completed in the first year.

2.2 Samples

The most common materials are cross-linked polyethylene (XLPE), ethylene propylene rubber (EPR), cross-linked polyolefin (XLPO), silicone rubber (SR), chlorosulfonated polyethylene (CSPE), ethylene tetra- fluoroethylene (ETFE), polyvinylchloride (PVC) and polyethylene (PE) are used for insulating and jacket materials in NPPs [4, 10], so a wide variety of cables were involved in the research work:

- XLPE/CSPE: single core, unshielded, XLPE insulated, CSPE jacketed cable manufactured by RSCC Wires, USA.
- EPR/CSPE: two-core, shielded, EPR insulated, CSPE jacketed cable manufactured by JS Cable, Korea.
- EPR/XLPO: seven-core, shielded, EPR insulated, XLPO jacketed cable manufactured by LS Cable, Korea.
- XLPO: unshielded single core XLPO insulated and jacketed photovoltaic DC cable from a non-specific manufacturer.
- PVC: PVC insulated and jacketed cables with various structures from non-specific manufacturers.

The Korean and RSCC cables were qualified as Class 1E LOCA cables, while the XLPO and PVC cables were general types. Although PVC insulated are not allowed to be installed in new nuclear facilities, investigating these cables has paramount practical importance because of the license or second license renewal of existing reactors. Besides the cable samples, PVC material samples were prepared with different plasticizer content to investigate the effect of cyclic thermal stress.

2.3 Ageing

Of the many stresses in reactors, radiation and elevated temperatures most significantly impact cable ageing [4, 8]. Therefore the standards only prescribe the application of these stress during accelerated ageing that simulates operation conditions [11]. Nevertheless, the low bending radius of cables can appear in some places in NPPs, affecting the cable insulation lifetime [12]. Since mechanical stress also degrades the insulating materials. [7]. Based on these considerations, the samples were exposed to the following accelerated ageings:

- Thermal ageing at different temperatures

- γ -irradiation ageing with different dose-rates.
- Combined mechanical and thermal ageing by bending the samples.
- Combined mechanical and γ -irradiation ageing by bending the samples.
- Repetitive thermal ageing with short-term cycles.

The parameters of the ageing programs are detailed in the section 2.4 Results.

2.4 Results

2.4.1 XLPE/CSPE Single-Core Cable

This cable type was aged in four manners: thermal ageing, irradiation ageing, combined thermal and mechanical ageing and combined irradiation and mechanical ageing.

Thermal ageing

The cable samples were aged at 120°C temperature in a ventilated oven. The results of dielectric spectroscopy show an increasing trend of $\tan \delta$ with thermal ageing, especially at lower (1...500 Hz) frequencies [14, 15] The 100 Hz tan delta values show a good correlation with ageing and the results of EaB measurements [14, 16].

A non-destructive Shore D hardness was also tested. It also correlates well with ageing and low-frequency (1...10 Hz) tan delta values [15]. The EVR was also measured on the samples. The slope of return voltage was decreased at the beginning of the ageing, and then the values had no significant change, probably due to the measurement uncertainty [17]. To reduce the effect of measurement uncertainty, by assuming the dielectric response function to be a power function, the slopes of the return voltage were determined by fitting curves to the measurement results. These estimated slopes of return voltages exhibited a strong correlation with ageing [18] (Figure 1).

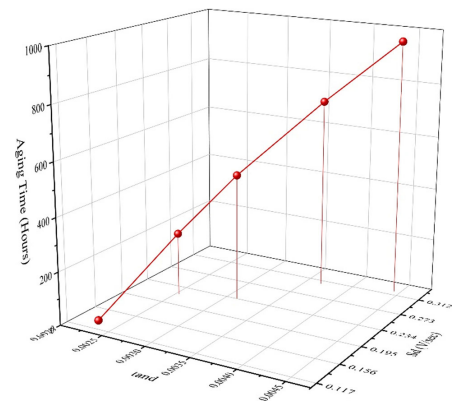


Figure 1: Trending of $\tan \delta$ and S_d with ageing times in hours [13]

Radiation ageing

The cable samples were aged by a ^{60}Co γ -ray source with a 0.5 kGy/h dose rate at Institute of Isotopes Ltd [19]. The real and imaginary parts of permittivity, calculated from the cable's geometry and the measured $\tan \delta$ and capacitance values, exhibited a solid increasing trend with the absorbed dose in the investigated frequency range (10 mHz...500 kHz).

At lower frequencies, i.e. below 10 Hz, this increment can be explained by the increased interfacial polarization. This cable structure is considered a layered insulation structure, and the interfacial polarization has a significant role in the low-frequency dielectric behaviour. The increment in the tens and hundreds of kHz range results from the intensity increase of orientation polarization because of the generation of dipolar byproduct due to ageing. The evaluation of dielectric spectrum curves is complicated, so derived quantities (figure) were introduced to characterize curves, making the comparison easier [20]. These deducted quantities are the $\tan \delta$ curve's central frequency and central loss factor. These quantities also correlate strongly with the ageing, indicating the increasing loss in the cable insulation in a wide frequency range. The central loss factor also correlates strongly with ageing, indicating the increasing loss in the cable insulation in a wide frequency range.

The increase in central frequency with ageing means that the dominant polarization became faster with ageing [21]. EVR measurements confirmed the increased intensity of interfacial polarization. Since the slope of return voltage was increased with the absorbed dose.

The slope of decay voltage was also increased due to the increasing conductivity of the samples.

The Shore D hardness of the samples was also increased with ageing. In addition, the electrical and mechanical parameters change shows a strong correlation.

The main findings are that the slope of return voltage and 100 Hz imaginary part of permittivity correlated well with ageing. Therefore these electrical parameters are good markers for non-destructive condition monitoring of this cable type [19] (Figure 2). Similar change can be observed the ac resistivity and strong correlation was observed between 100 Hz $\tan \delta$ and slope of decay voltage [13].

Combined thermal and mechanical ageing

The cable samples were subjected to successive thermal and mechanical ageing. The thermal ageing temperature was 120°C. After each ageing round, the samples were bent for two weeks. Comparing the dielectric spectroscopy measurement data with only thermally aged samples' data, the samples exposed to combined stress had higher $\tan \delta$ values, especially below 1000 Hz [22]. The imaginary part of permittivity was also higher in the case of samples subjected to the combined stresses in a wide frequency range [23].

The results of EVR measurement, i.e., slopes of decay and return voltages, were higher than those of only thermally aged samples [24]. These results can be explained by the intensity increment of interfacial polarization between the jacket and core insulation due to the bending of samples.

Samples were also prepared for simultaneous thermal and mechanical ageing by bending samples into a cylinder and heated to 120°C in an ageing chamber. The loss factor of samples below 10 Hz decreased, while above, it increased. Shore D was also tested, and a strong correlation was observed with $\tan \delta$ at 100 Hz [25]. Investigating the real and imaginary parts of permittivity in 0.1 Hz...500 kHz range, below 10 Hz, the imaginary part of permittivity decreased, above it increased with ageing time [26]. Measuring the EVR, the minimal slope of decay voltage increased, and the slope of return voltage decreased after 1 s shorting time decreased with ageing [26, 27].

The change of mechanical properties was tested by Shore D hardness. The high value of correlation coefficients calculated between mechanical and electrical properties makes the dielectric measurements capable of non-destructive condition monitoring [26] (Figure 3).

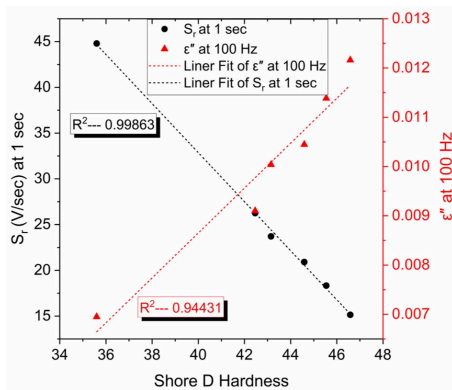


Figure 3: Correlation between S_r at 1 sec ϵ'' at 100 Hz, and hardness.[26]

Combined radiation and mechanical ageing

Bent cable samples were exposed to 0.5 kGy/h dose-rate irradiation for 400 kGy total dose [29]. The samples were measured by dielectric spectroscopy from 0.1 Hz to 1 kHz range, and the real and imaginary parts of permittivities were calculated. The real part of permittivity increased in the

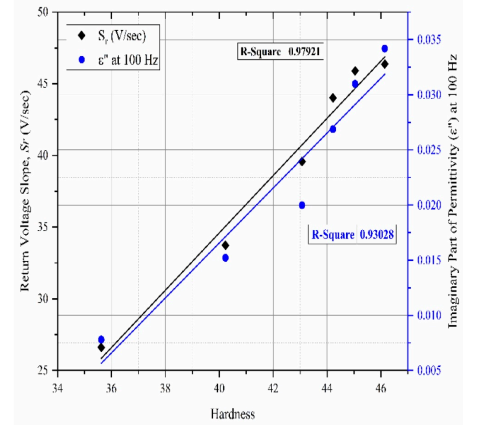
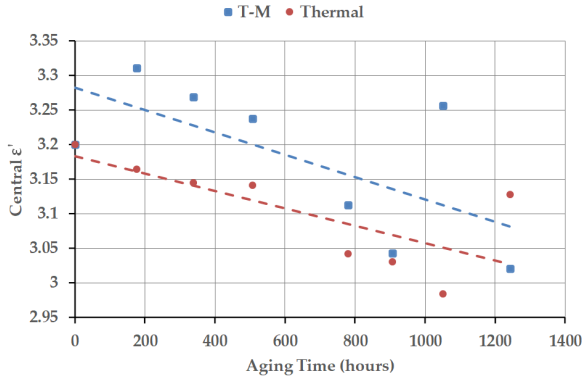
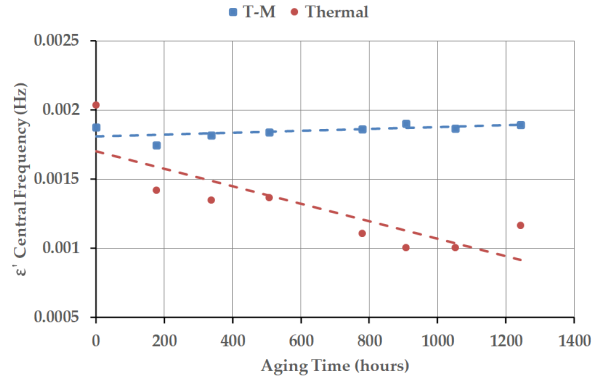


Figure 2: Correlation between S_r at 1 sec and change of ϵ'' at 10 Hz with Shore D hardness.[19]



(a)



(b)

Figure 4: The calculated deduced quantities to characterize the $\epsilon'(f)$ curves (a) central real part of permittivity (CRP); (b) real part of permittivity's central frequency (RPCF). [26]

investigated frequency range, while the imaginary permittivity curve shifted from the lower frequencies to the higher ones. Deducted quantities were also calculated, and a central frequency of the imaginary permittivity curves shifted towards higher frequencies with ageing.

Using a curve fitting method, an exponential curve described well the low-frequency change of the real and imaginary parts of permittivity in the case of combined ageing [30].

The intensity increase of interfacial polarization can explain this phenomenon. The jacket and the core insulation form a layered structure in a single-core cable. A change in the layers' dielectric properties (permittivity and conductivity) results in the intensity increase of the interfacial polarization. This phenomenon was proved by calculating the specific conductivity. Moreover, specific conductivity correlates well with the absorbed dose and the Shore D hardness of the cable insulation [30] (Figure 5).

Besides dielectric spectroscopy, the EVR was measured to investigate the time-domain dielectric response. The slopes of decay and return voltages showed increasing trends, as well. The Shore D hardness monotonously increases with the absorbed dose. The applicability of ageing markers for condition monitoring was tested by correlation calculation. The result revealed that the dielectric methods provide reliable ageing markers, strongly correlating with mechanical properties.

2.4.2 EPR/CSPE Insulated Two-Core Cable

This cable type were exposed to thermal, γ -irradiation and combined irradiation γ and mechanical ageing.

Irradiation ageing

The cable samples were irradiated with a 0.8 kGy/h dose rate. The total dose was 1200 kGy. The dielectric spectra of the samples were investigated in the 10 mHz to 500 kHz frequency range. The capacitance of the EPR insulation showed an increasing trend with absorbed dose, while the jacket's capacitance did not exhibit a clear trend. $\tan \delta$ of the core insulation also increased with ageing in the investigated frequency range. The jacket's $\tan \delta$ also had an increasing trend with an absorbed dose above 2 kHz. At lower frequencies, it had no clear trend.

The slopes of decay and return voltages also increased with ageing on the EPR insulation, while on the CSPE jacket, inconsistent changing of these values was observed.

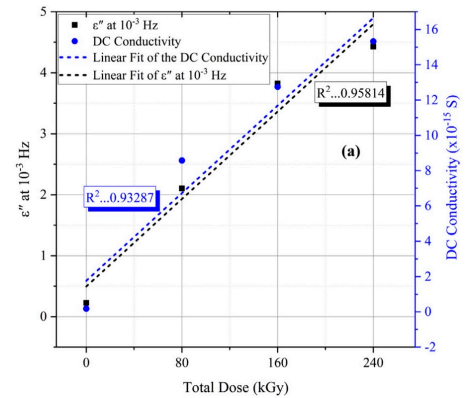


Figure 5: Correlation between ϵ'' at 1 mHz and the DC conductivity versus radiation dose [?]

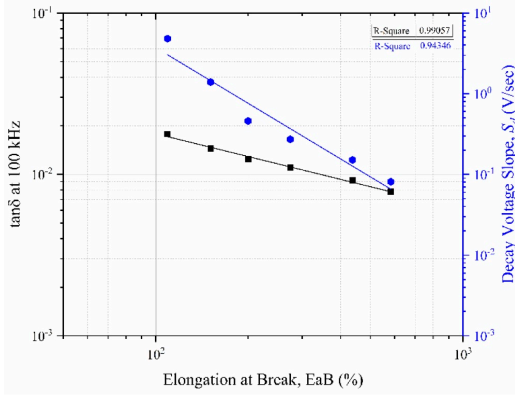
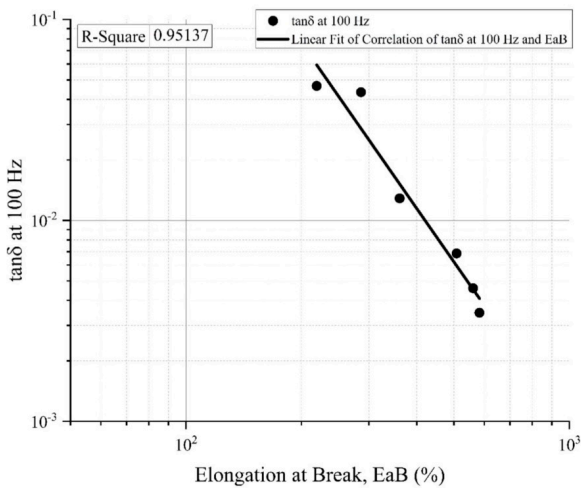
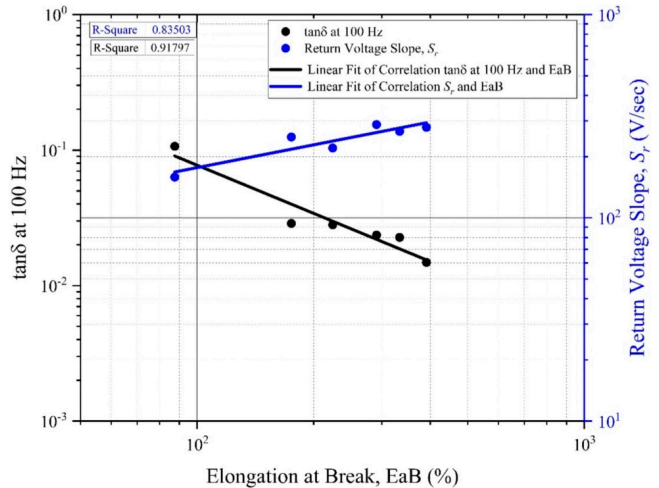


Figure 6: Correlation between elongation at break and (a) $\tan \delta$ at 100 kHz and S_d [31]

polarization-depolarization current (PDC) were also measured as time-domain dielectric response measurements. The slope of return voltage had to decrease trend with ageing in the case of the jacket, while other parameters on the jacket or the insulation did not show increasing or decreasing trends. The EaB of the jacket and insulation monotonously decreased with ageing time. However, they did not reach the 50% threshold value. The correlation between the dielectric parameters and EaB was tested. The 100 Hz $\tan \delta$ was also found as a good ageing marker for jacket and core insulation, showing a strong correlation with EaB, while the slope of return voltage for the jacket only (Figure 7) [32].



(a)



(b)

Figure 7: Correlation between $\tan \delta$ at 100 Hz: (a) EPR insulation and $\tan \delta$ at 100 Hz and S_r at 1 s and (b) CSPE jacket against EaB. [32]

The samples were also tested by the time-frequency domain reflectometry method. This method can locate the weakest points on a long cable section. Two assessment parameters, the peak value of envelope and the peak value of similarity, are defined and calculated from the reflected signal. After the ageing, the aged cable was connected to normal cables using a terminal, and the reflected signal from the terminal was used to extract the assessment parameters. As ageing time increases, the trend and linearity of the assessment parameters are clearly observed [33].

Combination of radiation and mechanical stresses

Straight and bent cable samples were irradiated by 0.8 kGy/h dose rate. The total dose was 1200 kGy. The dielectric spectrum was measured from 0.5 mHz to 1 kHz. The $\tan \delta$ values of cores were compared. The compression and stretch forces affected the core insulation since the cable is built up

from twisted cores. The results show that the tan delta values of mechanically stressed samples were higher in each ageing period than that of straightened ones, especially below 0.05 Hz and above 500 Hz. Comparing 1 mHz and 1 kHz tan delta values of both groups, the samples exposed to combined stresses have significantly higher values (Figure 8).

The investigation results suggest that mechanical stress has an important effect on ageing under irradiation. Therefore, this factor should be considered in the qualification procedure of nuclear cables [34].

2.4.3 PVC Insulated Cables

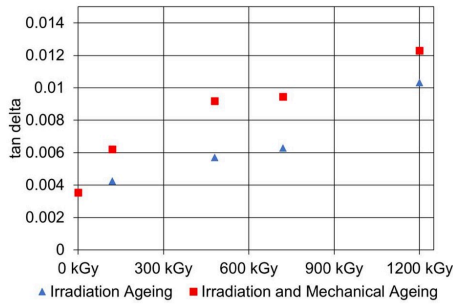


Figure 8: tan δ vs. total dose at 1000 Hz [34]

PVC cable samples were thermally aged at 110°C, 125°C and °C using 3-hour cycles. The change in the dielectric spectrum was investigated, and the EVR measurement was also carried out. Parallely, the Shore D hardness was tested. At the beginning of the ageing, softening of the material was observed. Later according to the expectations, the hardness was increased due to the plasticiser evaporation. The dielectric measurements followed this change, i.e., the slope of decay voltage and introduced deducted quantities to characterise the dielectric spectrum. The measurements on the PVC samples showed similar behaviour [35].

The effect of 6 hours thermal ageing cycles was also investigated on PVC-insulated LV cables. The tan δ , capacitance and PDC measurements were measured on the jacket and core

insulation.

It was seen that tan δ has increased with ageing. The capacitance of core insulation had also shown an upward trend, but the trend was not clear for the jacket. The polarisation current also increased, suggesting the increase in the conductivity of the PVC material [36, 37].

Since the mechanical and electrical parameters of PVC insulating material show an unclear trend during cyclical ageing of PVC cables [35]. In [38], the effect of the structure was investigated to reveal whether the behaviour due to repetitive ageing is a characteristic of the polymer itself or whether it results from the structure as well. Therefore three samples were prepared by removing different layers (outer jacket, jacket and steel armour, and jacket, steel armour and PPVC belting layer) from the cable and aged them with an intact cable sample.

Tan δ , capacitance and PDC measurements were executed, and Shore D hardness was tested on the inner PVC belting layers of samples. The results showed that the outer jacket's pressure significantly affected the conductive current, resulting in the high low-frequency tan δ . The high-frequency tan δ also showed similar behaviour [39]. It was confirmed by the calculated conductive current from PDC measurement. Another important finding of the comparison of the dielectric parameters after the structure change is that the capacitance measurements showed that the PVC belting layer was the most dominant component in the dielectric behaviour of this kind of cable. Another important finding is that the PVC belting layer is important in plasticizer evaporation. This layer provided enough protection from the environmental air since after removing this layer, the plasticizer evaporation occurred more easily. The results of the Shore D hardness measurement also proved this, as well as the conductive current correlation with the Shore D hardness of the belting layer (Figure 9).

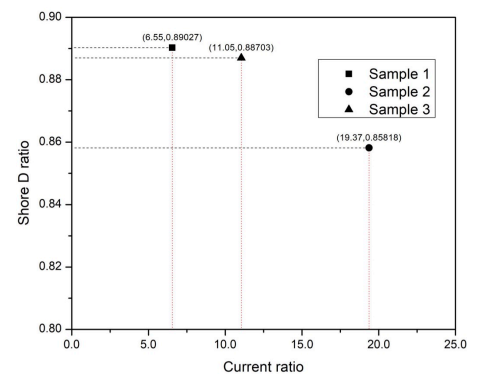


Figure 9: Comparison of the Shore D hardness and the conduction current after and before aging ratios. [38]

2.4.4 EPR/XLPO Insulated Multicore Cable

The cables used in nuclear power plants have various structures, especially the I&C cables containing multiple cores. Therefore, dielectric testing measures the resultant dielectric properties of the materials inside the cable; hence, the measurements' results can differ from core to core. Nevertheless, the measurement time for one cable is limited, so measuring all cores in a given cable is impossible. Therefore it is particularly important to recommend which cores should be measured for condition monitoring in the case of multicore cables aged under the same conditions. The cable samples were exposed to γ irradiation for accelerated ageing. The dose rate was 0.8 kGy/h, and the total absorbed dose was 1200 kGy. The dielectric properties were measured between 0.5 mHz and 5 kHz. The $\tan \delta$ values compared the central and one outer core. The results showed a relatively big difference in the measured $\tan \delta$ values in almost all the measuring frequencies after each ageing cycle. Only at 4.4 kHz, 5.0 kHz frequencies and in the 40-110 Hz frequency range, lesser this difference than 25%. Therefore during regular condition monitoring measurements, the same cores must be measured in a given cable; the measured cores cannot be changed [40].

The correlation with ageing was also tested on both cores. The results showed that in the central core case, the 0.46...4.64 mHz and 2.24 kHz frequency $\tan \delta$ values correlate well with ageing. The outer core's $\tan \delta$ correlates with ageing between 2.15 mHz and 0.22 Hz.

By averaging the results of outer and central cores, the outlier data effect on the results is decreasing, so in addition to the low-frequency $\tan \delta$ results, a solid trend was observed in the change of $\tan \delta$ at 1.00 kHz and 2.4 kHz (Figure 10).

Fortunately, at higher frequencies (in the kHz range), loss factor measurements do not require as long a time as at mHz frequencies. Thus, it is advisable to measure the loss factor on several cores and make a diagnostic decision based on the average loss factor values of the cores.

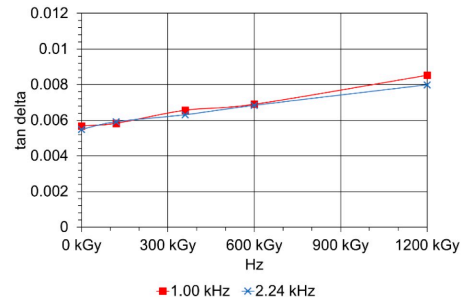


Figure 10: Changing of the loss factor measured at the two frequencies with the highest R^2 values as a function of absorbed dose in the kHz range [40]

2.4.5 XLPO Insulated Single-Core Cable

This cable type was exposed to combined thermal and mechanical ageing [41]. The ageing temperature was 120°C, and the samples were bent to a 6 cm outer diameter cylinder. The complex permittivity values were calculated from the dielectric spectroscopy measurement in 100 mHz...500 kHz. The time domain dielectric response was measured by the EVR method, and Shore D hardness was also tested.

After the first ageing cycle, the real and imaginary parts of permittivity decreased after these parameters were increased. Since XLPO is a semi-crystalline material, this behaviour can result from the material's recrystallisation. A similar trend was observed in the hardness and the decay voltage slope. The real and imaginary parts of permittivities agreed well with the decay and return voltage slopes. This result elucidates the applicability of these parameters to assess the ageing of polymers [42].

2.5 Dielectric modelling of ageing processes — *unpublished results*

The modelling of the dielectric response of insulations during ageing can help to understand the degradation mechanisms of insulating materials. These models can be useful in the prediction of the end of a lifetime based on establishing the relationship between mechanical properties (especially E_aB) and dielectric measurements. The developed dielectric model was based on the measurement results of EVR. This modelling highlights the advantage of this method, developed in this project (see Section 2.1).

2.5.1 The developed model

The degradation of polymers affects the dielectric properties such as conduction and polarization. The slow polarization processes, which can be investigated by the developed EVR technique, are usually related to space or interfacial elementary polarization processes [43]. These processes are the result of the electron trapping and de-trapping mechanisms. The de-trapping of electrons in a charged polymer leads to an isothermal relaxation current, and according to the theory of Simmons and Tam, this current function can be expressed as [44]:

$$j(t) = \frac{eLk_B T}{2t} f_0(E)N(E), \quad (1)$$

where e is the electron's charge, L is the thickness of the insulation k_B the is the Boltzmann's constant, T is the absolute temperature, $f(E)$ is the initial distribution of traps, $N(E)$ is the trap density.

It can be deduced that the slope of return voltage after t discharging time ($S_r(t)$) will be proportional to the $j(t)$. Hence from the results of EVR measurement, the electron trap distribution can be determined. Since there are more traps with different depths in the dielectric, the $S_r(t)$ will also be the sum of de-trapping currents with different depths. Assuming two electron traps (shallow and deep traps), the $S_r(t)$ was approximated by the sum of two exponentials (Debye model):

$$S_r(t) = A_1 e^{-t/\tau_1} + A_2 e^{-t/\tau_2}, \quad (2)$$

where A_1 and A_2 are the intensities, and τ_1 and τ_2 are the time constants of the Debye processes.

For calculations SciPy scientific computing library for the Python was used [45].

$$0.1 < A_1, A_2 < 100$$

$$0.3 < \tau_1, \tau_2 < 10000.$$

2.5.2 Results

The proposed method was tested on two-core EPR/CSPE samples exposed to thermal ageing, irradiation by different doses and combined radiation-mechanical ageing.

Ageing by irradiation

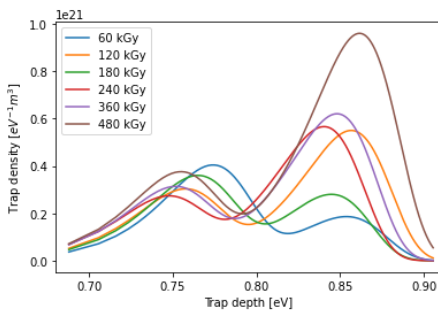


Figure 12: Trap density of irradiated samples by 0.1 kGy dose rate

beginning of the irradiation [46]. Due to the dose rate effect, it disappeared at a lower total dose in the case of low dose rate irradiation.

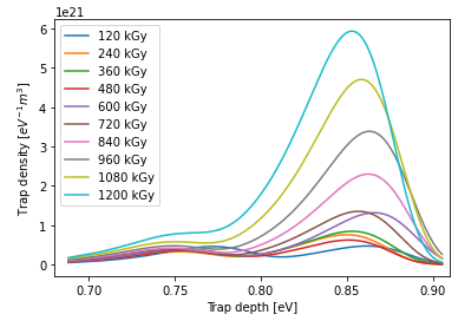


Figure 11: Trap density of irradiated samples by 0.8 kGy dose rate

The modelling tool was executed on two samples with 0.8 kGy/h and 0.1 kGy/h dose-rate irradiation.

In the case of samples with higher irradiation dose rates, the density of deep traps was increased with the absorbed dose (Figure 11).

Compared with the results of the low dose rate irradiated samples, except in the case of 480 kGy absorbed dose samples, the higher dose rate irradiated samples have higher trap densities (Figure 12).

It can also be observed that in both dose rates at the beginning of the ageing, there was no significant increase in trap densities. A clear trend is seen after 720 kGy in the case of high dose rate, while after 360 kGy in the low dose rate case. This phenomenon can be explained by the onset of reticulation at the

Combination of radiation and mechanical stresses

These samples were bent around a cylinder and exposed to 0.8 kGy/h irradiation. The results are depicted in Figure 13. Till 480 kGy dose, the mechanically stressed samples' deep trap density exceeded that of only irradiated ones. The ageing behaviour of EPR can explain it. During γ -irradiation, the chain scission and cross-linking occur parallel in the EPR insulating material. While chain scission generates traps, the cross-linking reduces trap densities. At the beginning of the ageing, due to mechanical stress, the chain scission is the dominant reaction. Later the free radicals, the products of chain scission, migrate to the interface of the crystalline/amorphous regions, where they initiate oxidation reactions, decreasing the number of electron traps [47].

Thermal ageing

The samples were exposed to thermal ageing at 120C. The trap density of samples with different ageing hours is in Figure 14. The deep trap density (0.85 eV) was increased, even not monotonously, during ageing, while the shallow trap density decreased after the first ageing cycle but later exhibited a solid increasing trend. This kind of behaviour of electrical properties was observed previously in the thermal ageing of EPR insulating material [48].

Conclusion

Based on the examination results, it can be concluded that in all cases, independently of the ageing stressor, shallow and deep trap depths are around 0.75 eV and 0.85 eV, respectively. However, it can also be noted, also the shallow and deep trap densities increased with ageing, although not monotonically in all cases. This can be explained by the fact that the same reactions are taken place in the degradation process of EPR independently of the ageing stressor. Nevertheless, different reactions are responsible for EPR ageing, Therefore similar ageing processes are taken place in the material. However, which reaction is dominant depends on the stress, their intensity and their combination. Nevertheless, comparing the trap densities with the results of EaB measurements, it can be stated that if the deep trap density reaches the $10^{21} eV^{-1} m^{-3}$, the value of EaB is also close to the threshold limit. Hence by the trap density, the cables can be sorted by condition.

This section results are prepared for publication as an IEEE Transactions paper.

3 Project Personnel

At the beginning of the project, it was planned to have the non-electrical measurements carried out by an external contractor. Contrary to the project proposal, we finally managed to carry out these measurements with the help of BME researchers, mostly from the Laboratory of Plastics and Rubber Technology. This cooperation became a fruitful professional relationship, resulting in another successful OTKA proposal (FK142814).

Particularly worth highlighting, numerous students (Jin Jizhu, Ritter Bence, Nouini Oumaima, Chrikioui Zakaria, Demkó Bettina, Deli Boglárka Orsolya, Liu Fang, Asipuela Gonzalez Angel Gabriel, Rusznyák Cintia and Spisák Alexa) were involved in the project, and they successfully defended their BSc and MSc theses relating to the project's topic.

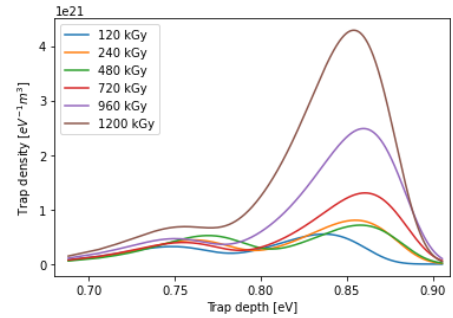


Figure 13: Trap density of samples exposed to combined, mechanical and radiation ageing.

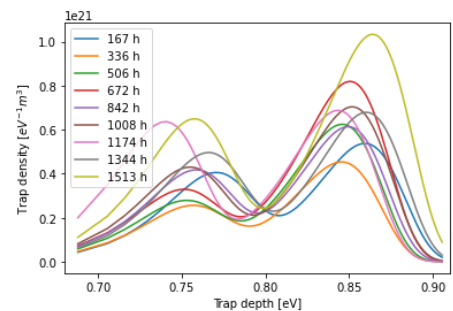


Figure 14: Trap density of thermally aged samples.

Three students (Csányi Gergely Márk, Ehtasham Mustafa and Ramy S. A. Afia) successfully defended their PhD theses on scientific results directly related to the project.

4 Practical application of the results

The research work has clearly demonstrated that the method developed is suitable for the non-destructive condition determination of aged cable samples subjected to laboratory ageing. The next step should be to test the method's applicability in the field. Since the principal investigator was involved in several R&D projects also with MVM Paks Nuclear Power Plant Ltd. and Paks II Nuclear Power Plant Ltd., it was agreed with experts from both companies to share the results of the project in a workshop this fall. Moreover, the possibility of operational testing of the developed method will be discussed.

References

- [1] IEA, "Nuclear power and secure energy transitions." International Energy Agency, Paris, <https://www.iea.org/reports/nuclear-power-and-secure-energy-transitions>, June 2022.
- [2] IEA, "Nuclear power in a clean energy system." International Energy Agency, Paris, <https://www.iea.org/reports/nuclear-power-in-a-clean-energy-system>, May 2019.
- [3] IEC/IEEE, "60780-323-2016 – IEC/IEEE International Standard - Nuclear facilities – Electrical equipment important to safety – Qualification," 2016.
- [4] IAEA, *Benchmark Analysis for Condition Monitoring Test Techniques of Aged Low Voltage Cables in Nuclear Power Plants*. No. 1825 in TECDOC Series, Vienna: INTERNATIONAL ATOMIC ENERGY AGENCY, 2017.
- [5] H. M. Hashemian, B. Mcconkey, G. Harmon, and C. Sexton, "Methods for testing nuclear power plant cables," *IEEE Instrumentation & Measurement Magazine*, vol. 16, no. 5, pp. 31–36, 2013.
- [6] D. Fabiani, G. Mazzanti, S. V. Suraci, and B. Diban, "Innovative development and application of a stress-strength model for reliability estimation of aged lv cables for nuclear power plants," *IEEE Transactions on Dielectrics and Electrical Insulation*, vol. 28, no. 6, pp. 2083–2090, 2021.
- [7] R. S. A. Afia, E. Mustafa, and Z. Á. Tamus, "Mechanical stresses on polymer insulating materials," in *2018 International Conference on Diagnostics in Electrical Engineering (Diagnostika)*, pp. 1–4, 2018.
- [8] E. Mustafa, R. S. A. Afia, and Z. Á. Tamus, "Condition monitoring uncertainties and thermal - radiation multistress accelerated aging tests for nuclear power plant cables: A review," *Periodica Polytechnica Electrical Engineering and Computer Science*, vol. 64, no. 1, pp. 20–32, 2020.
- [9] Z. Á. Tamus, "Combination of voltage response method with non-contact electrostatic voltage measurement to determine the dielectric response of insulating materials," *Journal of Physics: Conference Series*, vol. 1322, no. 1, p. 012042, 2019.
- [10] L. Bustard and P. Holzman, "Low-voltage environmentally-qualified cable license renewal industry report: Revision 1 final report," Tech. Rep. EPRI-TR-103841, United States, 1994.
- [11] IEEE, "Ieee standard for qualifying electric cables and splices for nuclear facilities," 2015.
- [12] V. Plaček, T. Kohout, J. Kábrt, and J. Jiran, "The influence of mechanical stress on cable service life-time," *Polymer Testing*, vol. 30, no. 7, pp. 709–715, 2011.
- [13] E. Mustafa, R. S. A. Afia, and Z. Á. Tamus, "Dielectric loss and extended voltage response measurements for low-voltage power cables used in nuclear power plant: potential methods for aging detection due to thermal stress," *Electrical Engineering*, vol. 103, no. 2, pp. 899–908, 2021.

- [14] A. Asipuela, E. Mustafa, R. S. A. Afia, T. Z. Adam, and M. Y. A. Khan, “Electrical condition monitoring of low voltage nuclear power plant cables: $\tan\delta$ and capacitance,” in *2018 International Conference on Power Generation Systems and Renewable Energy Technologies (PGSRET)*, pp. 1–4, 2018.
- [15] E. Mustafa, R. S. A. Afia, and Z. Á. Tamus, “Investigation of electrical and mechanical properties of low voltage power cables under thermal stress,” in *2020 International Conference on Diagnostics in Electrical Engineering (Dagnostika)*, pp. 1–4, 2020.
- [16] E. Mustafa, R. S. A. Afia, S. Bal, and Z. Á. Tamus, “Study of electrical integrity of low voltage nuclear power cables in case of plant life extension,” in *Technological Innovation for Life Improvement* (L. M. Camarinha-Matos, N. Farhadi, F. Lopes, and H. Pereira, eds.), (Cham), pp. 311–318, Springer International Publishing, 2020.
- [17] E. Mustafa, T. Z. Ádám, R. S. A. Afia, and A. Asipuela, “Thermal degradation and condition monitoring of low voltage power cables in nuclear power industry,” in *Technological Innovation for Industry and Service Systems* (L. M. Camarinha-Matos, R. Almeida, and J. Oliveira, eds.), (Cham), pp. 405–413, Springer International Publishing, 2019.
- [18] R. S. A. Afia, E. Mustafa, and T. Z. Ádám, “Evaluation of thermally aged nuclear power plant power cables based on electrical condition monitoring and regression analysis,” in *2019 International IEEE Conference and Workshop in Óbuda on Electrical and Power Engineering (CANDO-EPE)*, pp. 203–206, 2019.
- [19] E. Mustafa, R. S. A. Afia, and Z. Á. Tamus, “Application of non-destructive condition monitoring techniques on irradiated low voltage unshielded nuclear power cables,” *IEEE Access*, vol. 8, pp. 166024–166033, 2020.
- [20] Z. Á. Tamus, B. Deli, B. Demkó, C. Rusznyák, and Y.-J. Shin, “Application of derived quantities from the results of general electrical tests for condition monitoring of nuclear power plant instrumentation and control cables,” in *FONTEVRAUD 9, Contribution of Materials Investigations and Operating Experience to Light Water NPPs Safety, Performance and Reliability*, 2018.
- [21] E. Mustafa, R. S. A. Afia, and Z. Á. Tamus, “Application of novel electrical aging markers for irradiated low voltage nuclear power plant power cables,” in *2020 IEEE 3rd International Conference and Workshop in Óbuda on Electrical and Power Engineering (CANDO-EPE)*, pp. 000069–000072, 2020.
- [22] R. S. A. Afia, T. Z. Ádám, and E. Mustafa, “Effect of combined stresses on the electrical properties of low voltage nuclear power plant cables,” in *Technological Innovation for Industry and Service Systems* (L. M. Camarinha-Matos, R. Almeida, and J. Oliveira, eds.), (Cham), pp. 395–404, Springer International Publishing, 2019.
- [23] R. S. A. Afia, E. Mustafa, S. Bal, and Z. Á. Tamus, “Investigating the complex permittivity of low voltage power cables under different stresses,” in *Technological Innovation for Life Improvement* (L. M. Camarinha-Matos, N. Farhadi, F. Lopes, and H. Pereira, eds.), (Cham), pp. 319–327, Springer International Publishing, 2020.
- [24] R. S. A. Afia, E. Mustafa, and T. Z. Ádám, “Non-destructive condition monitoring of nuclear power plant power cables,” in *2019 7th International Youth Conference on Energy (IYCE)*, pp. 1–4, 2019.
- [25] R. S. A. Afia, E. Mustafa, and Z. Á. Tamus, “Dielectric spectroscopy of low voltage nuclear power cables under simultaneous thermal and mechanical stresses,” *Energy Reports*, vol. 6, pp. 662–667, 2020.
- [26] R. S. A. Afia, M. Ehtasham, and Z. Á. Tamus, “Electrical and mechanical condition assessment of low voltage unshielded nuclear power cables under simultaneous thermal and mechanical stresses: Application of non-destructive test techniques,” *IEEE Access*, vol. 9, pp. 4531–4541, 2021.

- [27] R. S. A. Afia, E. Mustafa, and T. Z. Ádám, “Extended voltage response measurement of low voltage nuclear power cables under simultaneous thermal and mechanical aging,” in *2020 IEEE 3rd International Conference and Workshop in Óbuda on Electrical and Power Engineering (CANDO-EPE)*, pp. 000213–000216, 2020.
- [28] R. S. A. Afia, E. Mustafa, and Z. Á. Tamus, “Comparison of mechanical and low-frequency dielectric properties of thermally and thermo-mechanically aged low voltage cspe/xlpe nuclear power plant cables,” *Electronics*, vol. 10, no. 22, 2021.
- [29] R. S. A. Afia, E. Mustafa, and Z. Á. Tamus, “Aging mechanisms and non-destructive aging indicators of xlpe/cspe unshielded lv nuclear power cables subjected to simultaneous radiation-mechanical aging,” *Polymers*, vol. 13, no. 18, 2021.
- [30] R. S. A. Afia, E. Mustafa, and Z. Á. Tamus, “Aging assessment of xlpe/cspe lv nuclear power cables under simultaneous radiation–mechanical stresses,” *Energy Reports*, vol. 8, pp. 1028–1037, 2022.
- [31] E. Mustafa, R. S. A. Afia, O. Nouini, and Z. Á. Tamus, “Implementation of non-destructive electrical condition monitoring techniques on low-voltage nuclear cables: I. irradiation aging of epr/cspe cables,” *Energies*, vol. 14, no. 16, 2021.
- [32] E. Mustafa, R. S. A. Afia, A. Nawaz, O. Nouini, and Z. Á. Tamus, “Implementation of non-destructive condition monitoring techniques on low-voltage nuclear cables: Ii. thermal aging of epr/cspe cables,” *Energies*, vol. 15, no. 9, 2022.
- [33] G. Y. Kwon, Y. H. Lee, S. S. Bang, G. H. Ji, G. S. Lee, Z. Á. Tamus, and Y. J. Shin, “Assessment of cable aging for nuclear power plants i&c cable via time-frequency domain reflectometry,” in *2020 IEEE 3rd International Conference on Dielectrics (ICD)*, pp. 77–80, 2020.
- [34] Z. A. Tamus and O. Nouini, “Frequency domain spectroscopy analysis of epr/cspe insulated nuclear power plant cable samples subjected to irradiation ageing and combined irradiation and mechanical ageing,” in *2023 INSUCON - 14th International Electrical Insulation Conference (INSUCON)*, pp. 179–184, 2023.
- [35] G. M. Csányi, S. Bal, and Z. Á. Tamus, “Dielectric measurement based deducted quantities to track repetitive, short-term thermal aging of polyvinyl chloride (pvc) cable insulation,” *Polymers*, vol. 12, no. 12, 2020.
- [36] S. Bal and Z. Á. Tamus, “Investigation of effects of thermal ageing on dielectric properties of low voltage cable samples by using dielectric response analyzer,” in *2022 International Conference on Diagnostics in Electrical Engineering (Diagnostika)*, pp. 1–6, 2022.
- [37] S. Bal and Z. A. Tamus, “Analyzing the effect of thermal stress on dielectric parameters of pvc insulated low voltage cable sample,” in *2022 IEEE 5th International Conference and Workshop Óbuda on Electrical and Power Engineering (CANDO-EPE)*, pp. 000067–000072, 2022.
- [38] S. Bal and Z. Á. Tamus, “Investigation of the structural dependence of the cyclical thermal aging of low-voltage pvc-insulated cables,” *Symmetry*, vol. 15, no. 6, 2023.
- [39] S. Bal, A. G. N. A. Jasim, and Z. A. Tamus, “Analyzing the effect of thermal ageing on low voltage distribution cables in relation to their structure,” in *2023 INSUCON - 14th International Electrical Insulation Conference (INSUCON)*, pp. 209–214, 2023.
- [40] O. Nouini and Z. A. Tamus, “Ageing behaviour analysis of different cores of multicore nuclear power plant instrumentation and control cables by dielectric spectroscopy,” in *Jicable’23 — International Conference on Insulated Power Cables*, no. E6.4, 2023.

- [41] R. S. A. Afia, E. Mustafa, and Z. Á. Tamus, “Condition monitoring of photovoltaic cables based cross-linked polyolefin insulation under combined accelerated aging stresses: Electrical and mechanical assessment,” *Energy Reports*, vol. 8, pp. 1038–1049, 2022.
- [42] R. S. A. Afia, E. Mustafa, and Z. Á. Tamus, “Thermal-mechanical accelerated aging tests of xlpo insulation based photovoltaic cables: Inverse aging behavior,” in *2021 IEEE 4th International Conference and Workshop Óbuda on Electrical and Power Engineering (CANDO-EPE)*, pp. 31–36, 2021.
- [43] E. Mustafa, R. S. A. Afia, and T. Z. Adam, “A review of methods and associated models used in return voltage measurement,” in *2018 International Conference on Diagnostics in Electrical Engineering (Diagnostika)*, pp. 1–4, 2018.
- [44] J. G. Simmons and M. C. Tam, “Theory of isothermal currents and the direct determination of trap parameters in semiconductors and insulators containing arbitrary trap distributions,” *Physical Review B*, vol. 7, pp. 3706–3713, 04 1973.
- [45] P. Virtanen, R. Gommers, T. E. Oliphant, M. Haberland, T. Reddy, D. Cournapeau, E. Burovski, P. Peterson, W. Weckesser, J. Bright, S. J. van der Walt, M. Brett, J. Wilson, K. J. Millman, N. Mayorov, A. R. J. Nelson, E. Jones, R. Kern, E. Larson, C. J. Carey, Í. Polat, Y. Feng, E. W. Moore, J. VanderPlas, D. Laxalde, J. Perktold, R. Cimrman, I. Henriksen, E. A. Quintero, C. R. Harris, A. M. Archibald, A. H. Ribeiro, F. Pedregosa, P. van Mulbregt, A. Vijaykumar, A. P. Bardelli, A. Rothberg, A. Hilboll, A. Kloeckner, A. Scopatz, A. Lee, A. Rokem, C. N. Woods, C. Fulton, C. Masson, C. Häggström, C. Fitzgerald, D. A. Nicholson, D. R. Hagen, D. V. Pasechnik, E. Olivetti, E. Martin, E. Wieser, F. Silva, F. Lenders, F. Wilhelm, G. Young, G. A. Price, G.-L. Ingold, G. E. Allen, G. R. Lee, H. Audren, I. Probst, J. P. Dietrich, J. Silterra, J. T. Webber, J. Slavič, J. Nothman, J. Buchner, J. Kulick, J. L. Schönberger, J. de Miranda Cardoso, J. Reimer, J. Harrington, J. L. C. Rodríguez, J. Nunez-Iglesias, J. Kuczynski, K. Tritz, M. Thoma, M. Newville, M. Kümmerer, M. Bolingbroke, M. Tartre, M. Pak, N. J. Smith, N. Nowaczyk, N. Shebanov, O. Pavlyk, P. A. Brodtkorb, P. Lee, R. T. McGibbon, R. Feldbauer, S. Lewis, S. Tygier, S. Sievert, S. Vigna, S. Peterson, S. More, T. Pudlik, T. Oshima, T. J. Pingel, T. P. Robitaille, T. Spura, T. R. Jones, T. Cera, T. Leslie, T. Zito, T. Krauss, U. Upadhyay, Y. O. Halchenko, Y. Vázquez-Baeza, and S. . . Contributors, “Scipy 1.0: fundamental algorithms for scientific computing in python,” *Nature Methods*, vol. 17, no. 3, pp. 261–272, 2020.
- [46] J. F. Calmet, F. Carlin, T. M. Nguyen, S. Bousquet, and P. Quinot, “Irradiation ageing of cspe/epr control command electric cables. correlation between mechanical properties and oxidation,” *Radiation Physics and Chemistry*, vol. 63, no. 3, pp. 235–239, 2002.
- [47] A. Rivaton, S. Cambon, and J. L. Gardette, “Radiochemical ageing of epdm elastomers.: 2. identification and quantification of chemical changes in epdm and epr films γ -irradiated under oxygen atmosphere,” *Nuclear Instruments and Methods in Physics Research Section B: Beam Interactions with Materials and Atoms*, vol. 227, no. 3, pp. 343–356, 2005.
- [48] G. C. Montanari, “An investigation on the thermal endurance of epr model cables,” *IEEE Transactions on Electrical Insulation*, vol. 25, no. 6, pp. 1046–1055, 1990.